Available online at www.sciencedirect.com
ScienceDirect
Biochimica et Biophysica Acta 1777 (2008) 140–153
Biochimica et Biophysica Acta
BBA
www.elsevier.com/locate/bbabio

Access channels and methanol binding site to the $CaMn_4$ cluster in Photosystem II based on solvent accessibility simulations, with implications for substrate water access

Felix M. Ho *, Stenbjörn Styring

Molecular Biomimetics, Department of Photochemistry and Molecular Science, Ångström Laboratory, P.O. Box 523, Uppsala University, SE-751 20 Uppsala, Sweden

Received 21 June 2007; received in revised form 28 August 2007; accepted 29 August 2007
Available online 14 September 2007

Abstract

Given the tightly packed environment of Photosystem II (PSII), channels are expected to exist within the protein to allow the movement of small molecules to and from the oxygen evolving centre. In this report, we calculate solvent contact surfaces from the PSII crystal structures to identify such access channels for methanol and water molecules. In a previous study of the effects of methanol on the EPR split S_1-, S_3-, and S_0-signals [Su et al. (2006) *Biochemistry* 45, 7617–7627], we proposed that methanol binds to one and the same Mn ion in all S-states. We find here that while channels of methanol dimensions were able to make contact with the $CaMn_4$ cluster, only ^{3}Mn and ^{4}Mn were accessible to methanol. Combining this observation with spectroscopic data in the literature, we propose that ^{3}Mn is the ion to which methanol binds. Furthermore, by calculating solvent contact surfaces for water, we found analogous and more extensive water accessible channels within PSII. On the basis of their structure, orientation, and electrostatic properties, we propose functional assignments of these channels as passages for substrate water access to the $CaMn_4$ cluster, and for the exit of O_2 and H^+ that are released during water oxidation. Finally, we discuss the possible existence of a gating mechanism for the control of substrate water access to the $CaMn_4$ cluster, based on the observation of a gap within the channel system that is formed by Ca^{2+} and several mechanistically very significant residues in the vicinity of the cluster.

Keywords: Photosystem II; Channel; Solvent contact surface; Substrate water access; H^+ exit pathway; O_2 exit pathway

1. Introduction

Photosystem II (PSII) is the enzyme responsible for the oxidation of water to molecular oxygen during photosynthesis in algae, cyanobacteria and higher plants. This is an extremely demanding reaction, requiring very high redox potentials. The energy is provided by light, and the heart of the catalytic centre is the oxygen evolving centre, which consists of a $CaMn_4$ cluster and a nearby D1-Tyr 161 residue, Y_Z. At each photoexcitation event, the primary donor known as P680 is oxidised, passing an electron to the acceptor side of PSII. The $CaMn_4$ cluster then re-reduces P680 via Y_Z, and in so doing undergoes four oxidation steps before O_2 is released through oxidation of two water molecules. This step-wise oxidation process, the S-cycle, involves five intermediates known as the S-states, labelled S_0 to S_4. S_0 is the most reduced state, and each oxidation step advances the $CaMn_4$ to the next S-state, up to the transient S_4 state. Once the S_4 state is reached, spontaneous $S_4 \rightarrow S_0$ transition takes place, with the concomitant release of molecular oxygen, through which the cluster is reduced back to the S_0 state. It is believed that substrate water molecules bind to the $CaMn_4$ cluster early during the S-cycle, with molecular oxygen being released at the completion of each cycle (for reviews and specialised journal issues on PSII water oxidation, see [1–9]).

S-state-specific EPR signals have been extensively used to study the S-cycle, and we have recently published data on the

Abbreviations: PSII, Photosystem II; P680, the primary donor in PSII; Y_Z, tyrosine 161 of the PSII D1 polypeptide; EPR, electron paramagnetic resonance; ESEEM, electron spin echo envelope modulation; CW, continuous wave; EXAFS, extended X-ray absorption fine structure; ESE-ENDOR, electron spin echo–electron nuclear double resonance; FT-IR, Fourier transform infrared; NIR, near infrared; QM/MM, quantum mechanics/molecular mechanics

* Corresponding author. Tel.: +46 18 4716584; fax: +46 18 4716844.
E-mail address: Felix.Ho@fotomol.uu.se (F.M. Ho).

0005-2728/$ - see front matter © 2007 Elsevier B.V. All rights reserved.
doi:10.1016/j.bbabio.2007.08.009

effects of methanol on each of the so-called split EPR signals then known [10], and compared those with methanol effects on other EPR signals arising from all S-states (excepting S_4). It was concluded that methanol binds to one and the same Mn ion of the $CaMn_4$ cluster for all S-states, and that the different methanol sensitivities thus reflect the structural changes in the cluster during the S-cycle, rather than different binding sites.

In the first part of this study, we consider which Mn ion is the most likely to be the binding site for methanol by calculating solvent contact surfaces within the highest resolution crystal structure of the PSII protein currently available [11] and comparing these results with structural and spectroscopic data on the $CaMn_4$ cluster. In the second part of this study, analogous solvent contact surfaces are calculated for water to examine water accessibility in PSII, and functional assignments for the channels thus identified in terms of water, H^+ and O_2 transport to and from the $CaMn_4$ cluster are proposed. In addition, we compare our results with those very recently reported by Murray and Barber [12].

2. Materials and methods

2.1. Calculation of solvent contact surfaces

Calculations of solvent contact surfaces were performed in DS Visualizer® (v. 1.7, Accelrys Software Inc.). Except mentioned otherwise, the surfaces shown were calculated using the atomic coordinates from the PSII crystal structure by Loll et al. (3.0 Å, PDB ID 2AXT [11]). Only one monomer of the PSII dimer complex represented in the crystal structure file was used for calculations. The calculations were also performed on the PSII crystal structure by Ferreira et al. (3.5 Å, PDB ID 1S5L [13]), yielding similar results.

Calculation and analysis of the solvent contact surfaces for the investigation of solvent accessibility proceeded as follows. First, all atoms within a radius of 15 Å away from the surface of the $CaMn_4$ cluster were selected. Atoms lying outside this region were hidden but not deleted, so that their presence was still taken into account during calculations. A Connelly-type solvent contact surface was then generated using the DS Visualizer® software, which employs a numerical grid-based algorithm to find regions within the selected set of atoms where a spherical probe with a radius approximating that of the desired solvent would fit between neighbouring atoms. For the calculation of the solvent contact surface for methanol, a probe radius of 1.7 Å was used, whereas a probe radius of 1.4 Å was used for calculating the water solvent contact surface [14,15]. All points within the protein structure which are able to accommodate the probe are determined, and the solvent contact surfaces to the surrounding atoms are generated. Therefore, all regions within the protein where a solvent molecule of the dimensions of the probe could potentially fit into are identified, with no constraint of there also being a continuous and open connection to the exterior of the protein.

The solvent contact surfaces were visually examined to identify solvent accessible regions which constitute channels making contact with the $CaMn_4$ cluster. Each channel was then followed beyond the 15 Å sphere by extending the selection of atoms included in the generation of the solvent contact surface according to the path of the channel, until the protein surface is reached.

In all instances, the residue numbering in the Loll et al. structure (2AXT [11]) is followed here. Note in particular that for the PsbO and PsbV subunits, the 2AXT numbering is shifted +26 compared to the numbering used in the PSII structure by Ferreira et al. (1S5L [13]).

3. Results and discussion

3.1. Methanol-sized solvent channels

Many small molecules are able to bind to the $CaMn_4$ cluster, and methanol in particular has been much studied, as it causes detectable changes in spectroscopic signals (reviewed in [10]). Pulsed EPR has been useful for studying the nature of methanol binding to the cluster. Force et al. [16] employed ESEEM spectroscopy to demonstrate that methanol binds close enough to the $CaMn_4$ cluster to be a ligand to a Mn ion. This was recently extended by Åhrling et al. [17], who demonstrated that the strongest methanol binding was most likely to occur via a terminal Mn-OCH_3 motif. In this study, we turn to spatial considerations around the $CaMn_4$ cluster in order to decide which of the Mn ions is most likely to be the methanol binding site.

Given the tightly packed environment, access through the protein is likely to be restricted to certain channels in the secondary structure. Furthermore, as there are numerous amino acids that ligate the $CaMn_4$ cluster, it is expected that there would be limitations on where methanol could make contact with the cluster. To identify these regions of access and where methanol binding to the cluster could take place, Connelly-like solvent contact surfaces were generated for the 3.0 Å crystal structure of PSII (PDB 2AXT [11]) using a probe radius of 1.7 Å to approximate the size of methanol [14,15]. As methanol does not inhibit oxygen evolution even at high concentrations (3–5 M [16,18]), it is unlikely that it would displace amino acid ligands of either the Mn or Ca ions in the $CaMn_4$ cluster. Furthermore, it has been shown that methanol binds non-competitively to Mn with respect to substrate water [17]. Therefore we do not consider the situation where methanol might displace an amino acid ligand to bind to a Mn ion.

We first checked the validity of this computational approach for the identification of solvent accessibility by calculating analogous water contact surfaces for cytochrome *c* oxidase, using a probe radius of 1.4 Å. This was first performed on the earlier 2.8 Å resolution structure of the enzyme [19], where water molecules were not resolved, and then overlaying the resulting surface onto the 1.8 Å resolution crystal structure [20], where individual water molecules in the water/H^+ channel could be explicitly seen. Water molecules in the channel were indeed found to lie in spaces predicted by the surfaces to be able to accommodate water, confirming the robustness of this analysis (not shown).

The initial search range was a 15 Å radius volume extending from the $CaMn_4$ cluster (taken as a whole). Fig. 1 shows the results of this analysis. In the centre, the four Mn ions and the Ca ion are visible. The Mn ions are numbered ^{1}Mn to ^{4}Mn, in accordance with the nomenclature in the crystal structure [11]. The red-hatched areas indicate the regions in the protein where the methanol-sized probe could be accommodated. The white regions are either occupied by the protein, or are voids which are too small to fit the solvent probe. As the calculations search for all free space within the protein which is able to accommodate the probe, many small pockets of apparent access are seen. They represent small enclosed spaces within the protein which would fit a probe molecule, but for which there is no apparent access to the outside via any open channels. However, two much larger and longer continuous channels that made contact with Mn ions in the $CaMn_4$ cluster were identified. Both are wide enough for the passage of methanol, and they both lead all the way to the

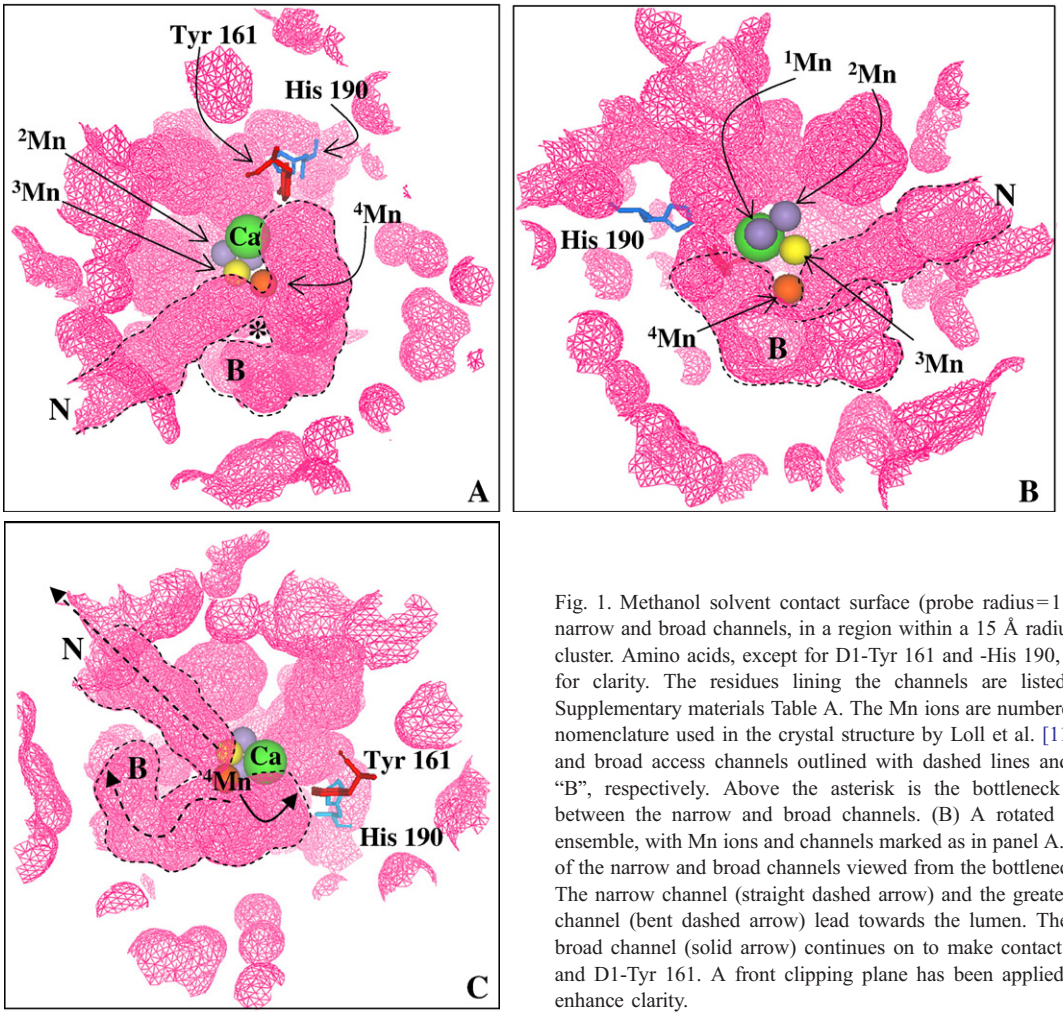

Fig. 1. Methanol solvent contact surface (probe radius = 1.7 Å) showing the narrow and broad channels, in a region within a 15 Å radius from the $CaMn_4$ cluster. Amino acids, except for D1-Tyr 161 and -His 190, have been omitted for clarity. The residues lining the channels are listed in Table 1 and Supplementary materials Table A. The Mn ions are numbered according to the nomenclature used in the crystal structure by Loll et al. [11]. (A) The narrow and broad access channels outlined with dashed lines and marked "N" and "B", respectively. Above the asterisk is the bottleneck forming the link between the narrow and broad channels. (B) A rotated view of the same ensemble, with Mn ions and channels marked as in panel A. (C) The directions of the narrow and broad channels viewed from the bottleneck junction at ^{4}Mn. The narrow channel (straight dashed arrow) and the greater part of the broad channel (bent dashed arrow) lead towards the lumen. The remainder of the broad channel (solid arrow) continues on to make contact with the Ca^{2+} ion and D1-Tyr 161. A front clipping plane has been applied to these views to enhance clarity.

$CaMn_4$ cluster (Fig. 1), thereby providing potential access channels for methanol.

Viewing the narrower of the two channels ("N") from the distal to the proximal end with respect to the $CaMn_4$ cluster, it can be seen that it first makes contact with ^{3}Mn before continuing on to make contact with ^{4}Mn (Fig. 1A). It does not come into contact with ^{1}Mn, ^{2}Mn or the Ca ion. This channel takes a fairly straight path towards the lumen, without significant bending. By contrast, the other channel ("B") is broader, and ^{4}Mn is the only Mn ion with which it makes contact. It is also more bent than the narrow channel. Following the path of this broad channel from the $CaMn_4$ cluster outwards, it takes two directions (Fig. 1A and C). Starting from where it makes contact with ^{4}Mn, approximately two-thirds of this channel extends away from the $CaMn_4$ cluster towards the luminal side of PS II (bent dashed arrow in Fig. 1C). The other branch of the channel bends back towards the cluster itself to make contact with the Ca^{2+} ion of the cluster, as well as $Y_Z^{\bullet}$ (solid arrow in Fig. 1C). The narrow and broad channels are joined at a bottleneck region which cradles ^{4}Mn (Fig. 1A and B). Positioned opposite ^{4}Mn at this junction between the two channels is the D1-Asp 61 residue. The amino acid residues lining the channels are listed in Table 1. A more detailed table including comparisons of these residue with those involved in channels as identified in [12], as well as listing the incidences of potential hydrogen bond acceptors making contact with the channels is presented in Supplementary materials Table A.

A third channel which made contact with the $CaMn_4$ cluster was also identified. However, unlike the other two, this channel did not make contact with the Mn ions of the $CaMn_4$ cluster, but rather made contact with the Ca^{2+} ion (Fig. 2). By comparison with the other two channels, this channel runs along the back of the cluster. The amino acid residues lining this "back channel" within a 15 Å radius from the $CaMn_4$ cluster are listed in Table 1, with a more detailed and complete list being presented in Supplementary materials Table B.

While this channel does not itself make contact with the Mn ions, it does make a very close approach to the broader of the two channels described above. This occurs at the Ca^{2+} ion (Fig. 2B). At this point, a small gap separates this back channel from the proximal end of the broad channel. The residues surrounding this gap are D1-Tyr 161, -His 190, -Glu 189, -Phe 186 and Gln 165, as well as the Ca^{2+} ion. This is particularly interesting given that these residues are proposed to be of special importance in

Table 1
Amino acid residues lining the narrow channel, the broad channel, the back channel and the large channel system

Narrow channel	Broad channel	Back channel	Large channel system
D1-Asp 61	D1-Ile 60	D1-Asn 87	D1-Glu 189
-Gly 62	-Asp 61	-Ala 88	-Glu 329
-Ile 63	-Ile 63	-Ile 89	-His 332
-Asn 87	-Glu 65	-Gly 90	-Pro 340
-Glu 333	-Val 67		
-Ser 169	-Pro 84	-Leu 91	-Leu 341
-Asn 335	-Tyr 161	-Tyr 161	-Asp 342
-Ala 336	-Ser 169	-Ile 163	-Leu 343
-Asn 338	-Asp 170	-Gly 164	-Ala 344
CP43-Pro 334	-Gly 171	-Gln 165	CP47-Arg 384
-Thr 335	-Met 172	-Gly 166	CP43-Glu 354
-Leu 337	-Pro 173	-Glu 189	-Met 396
-Met 342	-Asn 181	-His 190	-Ala 399
-Gly 353	-Phe 182	-Asn 296	-Leu 401
-Glu 354	-Val 185	-Asn 298	-Gly 409
-Met 356	-Phe 186	-Asp 342	-Val 410
-Arg 357	-Met 331	-Leu 343	-Thr 412
	-His 332	-Ala 344	-Glu 413
	-Glu 333	CP43-Trp 291	D2-Arg 348
	-Arg 334	-Phe 292	-Ala 351
	D2-Glu 312	-Gly 306	-Leu 352
	-Phe 314	-Phe 307	PsbU-Tyr 133
	-Lys 317	-Ala 309	PsbV-Lys 160
	-Leu 320	-Met 356	
	-Leu 321	-Arg 357	
		-Phe 358	
		-Ala 399	
		-Pro 400	
		-Leu 401	

In the interest of conciseness, only residues that are within a 15-Å radius from the $CaMn_4$ cluster (i.e., the initial search radius for modelling) are listed. The residues listed for the narrow, broad and back channels are implicated in both the methanol and water accessibility surfaces (D1-Asp 59 is also accessible from the broad channel when a water size probe is used). For a complete and more detailed list of all the residues making contact with the full-length channels, as well as the residues forming the extended narrow channel for the water accessibility surface, see Supplementary materials Tables A–D.

water oxidation, acting variously as oxidisers, proton acceptors and being part of a hydrogen-bonding network near the $CaMn_4$ cluster (reviewed in [21,22]; see also recently [23]). Possible implications of this are considered below.

Whereas ^{3}Mn and ^{4}Mn show close proximity to the narrow and broad channels, none of the channels identified makes contact with either ^{1}Mn or ^{2}Mn (Fig. 1B). These two ions were well separated from any solvent contact surface, reflecting the tight amino acid ligand environment around them. Therefore, based on the current medium-resolution PSII crystal structure, either ^{3}Mn or ^{4}Mn is the most likely candidate for the site of methanol binding in the $CaMn_4$ cluster.

3.2. Identity of the methanol binding site

Having concluded from the solvent accessibility calculations that ^{3}Mn and ^{4}Mn are both likely to be accessible to methanol, spectroscopic data in the literature were considered to further evaluate which of the two would be the more likely site of methanol binding. Two characteristics that have been attributed to methanol binding were relied on for this assessment: firstly, that binding occurs on one and the same Mn ion in the $CaMn_4$ cluster across the S-states, and secondly, that the binding Mn ion is likely to be in the 3+ oxidation state, at least in the S_2 state. These are discussed in turn below.

Two sets of spectroscopic studies have indicated that methanol binds to the same Mn ion in all S-states. In Su et al. [10], the effect of methanol on the split S_1-, S_3-and S_0-split signals was studied. By comparing the methanol concentration dependence of the spectral changes in the split signals as well as the S_2 and S_0 multiline signals [24], it was found that the S_1- and S_2-state EPR signals had similar methanol sensitivities, whereas significant differences were found upon $S_2 \rightarrow S_3$ and $S_0 \rightarrow S_1$ transitions. This seemed to correlate well with the available EXAFS data which have indicated that no significant structural changes occur in the $CaMn_4$ cluster during the $S_1 \rightarrow S_2$ transition, whereas such changes were observed for the $S_2 \rightarrow S_3$ and $S_0 \rightarrow S_1$ transitions [25,26]. Combining this with the observation that methanol addition had the general effect of increasing the energy gap between the ground and first-excited spin states in the $CaMn_4$ cluster, it was concluded that methanol binds to one and the same Mn ion across the S-states, with the differences in methanol sensitivity reflecting structural changes in the $CaMn_4$ cluster. This conclusion is consistent with ESSEM studies which have demonstrated that methanol binds directly to the $CaMn_4$ cluster in the S_2 [16,17] and S_0 states [17]. In addition, Åhrling et al. [17] have also proposed that methanol binds to the same Mn ion in the cluster across all the S-states. This conclusion was reached by taking into account the large spin projection coefficient ρ of ~ 2 for the methanol-binding Mn ion, the width of the multiline signals, and the fact that the same S_2 multiline EPR signal is obtained even when it is induced by illumination of the S_1 state at 200 K instead of direct single flash turnover to the S_2 state at room temperature.

The identification of the Mn ion to which methanol binds can then proceed on the basis of the oxidation state of the ion. EPR studies have suggested that the Mn ion to which methanol binds would be in a 3+ oxidation state in the S_2 state. In a CW- and ESEEM study of the S_2 multiline EPR signal, Åhrling et al. [27] noted the existence of two forms of the signal, one narrow and one broad, which were formed to varying relative proportions in the presence of methanol. This is in contrast to samples in the absence of methanol, where only the broad form of the S_2 multiline signal was found. The existence of these two forms when methanol was present could be explained by the fact that Mn(III) ions often undergo axial Jahn-Teller distortion, giving two possible ground configurations, $^5B_1$ and $^5A_1$, depending on whether axial ligation is weak or strong, respectively. Since a conversion of this Mn(III) ion from a $^5B_1$ symmetry to a $^5A_1$ symmetry would be sufficient to narrow the powder hyperfine pattern of the multiline signal, it was argued that methanol binds to this Mn(III) ion, and predisposes it to undergo a symmetry "flip", hence giving rise to the narrow and broad forms of the split signals in the presence of methanol.

This assignment of a Mn(III) binding site for methanol is in addition consistent with the loss of sensitivity to NIR radiation in the S_2 state. In the absence of methanol, NIR irradiation at

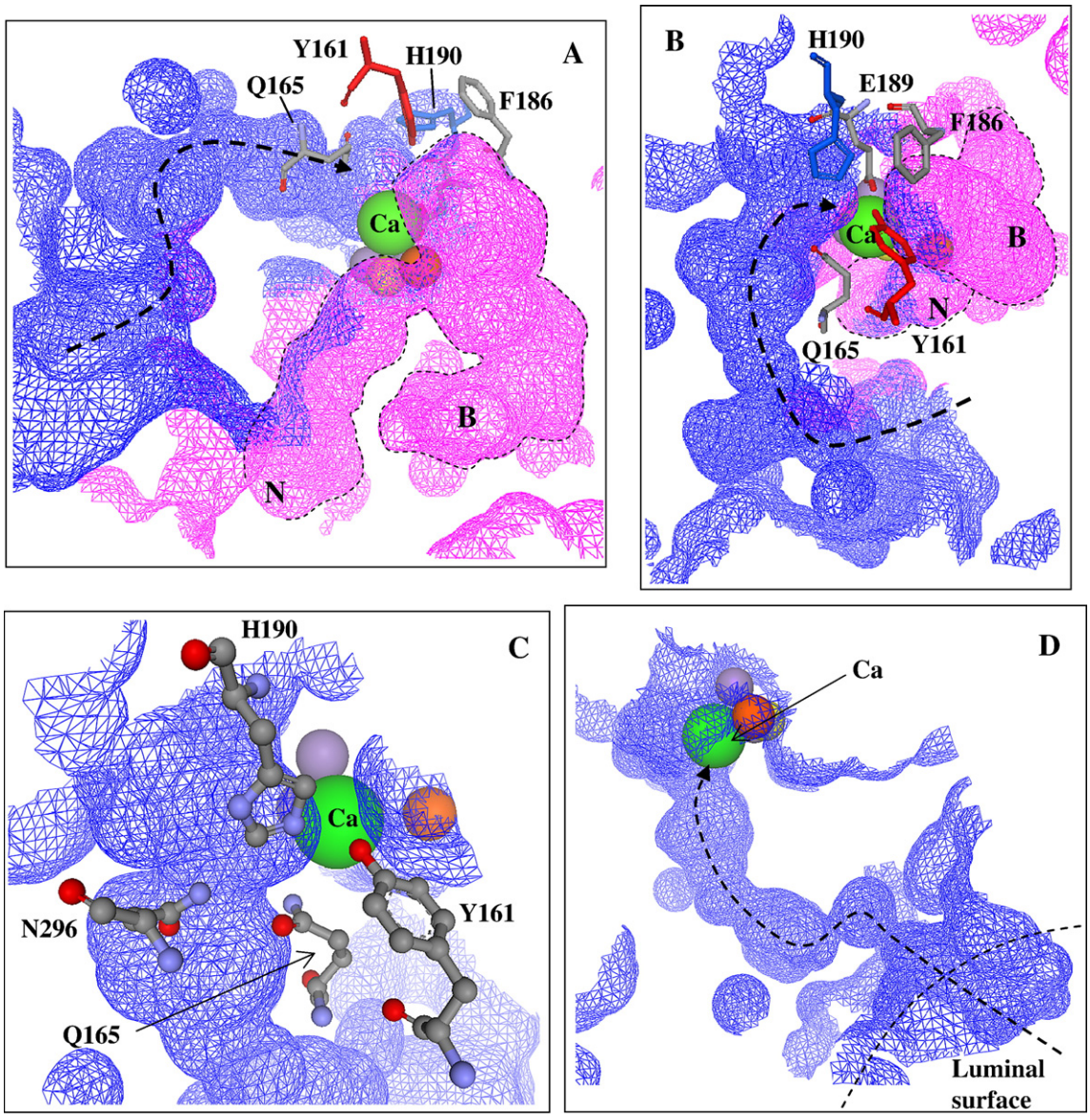

Fig. 2. The back channel in the methanol solvent contact surface (probe radius = 1.7 Å). All labelled residues originate from the D1 subunit. The residues lining the channel are listed in Table 1 and Supplementary materials Table B. (A and B) The back channel surface is coloured blue to distinguish it from the narrow ("N") and broad ("B") channels (pink). The dashed arrows show the possible access of molecules from the luminal side of the PSII membrane. The narrow and broad channels are outlined with dashed lines for guidance. Panel B is a rotated view of the same ensemble as shown in panel A to highlight the gap between the back and broad channels. In both panels A and B, the residues rendered in stick representation are the amino acids surrounding the gap between the back and broad channels (see text for details). In particular, D1-Tyr 161 (Y_Z) and -His 190 are highlighted in red and blue, respectively. Panel C shows the network of residues at the top of the back channel with potential hydrogen-bonding acceptors pointing towards the channel (blue atoms: N; red atoms: O). Panel D shows that the back channel extends to the luminal surface. The dashed arrow again represents the path of the channel, open from the luminal surface to the $CaMn_4$ cluster. In all panels, ^{3}Mn and ^{4}Mn are coloured yellow and orange, respectively.

temperatures <200 K of a sample poised in the S_2 state leads to the appearance of the broad $g \approx 4.1$ signal together with a reduction in multiline signal intensity. This conversion does not take place in the presence of methanol [24,28,29]. This NIR-induced process has been attributed to a spin conversion of the $CaMn_4$ cluster from $S = 1/2$ to $S \geq 5/2$ [30,31], possibly due to either a change in the identity of the Mn(III) ion within the cluster (e.g., through intra-cluster charge transfer where a Mn (III) ion reduces a neighbouring Mn(IV) ion to Mn(III): [32,33]), a d–d transition [34,35], or a high-spin to low-spin conversion of the Mn(III) ion [36]. Therefore, the fact that sensitivity of the S_2 state towards NIR radiation is lost upon methanol addition further strengthens the case for a Mn(III) as the binding ion.

Summing up the spectroscopic information so far, the Mn ion to which methanol binds is one and the same across the S-states, and is in particular in the 3+ oxidation state in the S_2 state. The existence of at least one Mn(III) ion in the S_2 state is accepted in the literature, with a 3Mn(IV)1Mn(III) configuration in the S_2 state being favoured by most authors [2,25,26,37–39]. In the present context, it is moreover interesting to note that in the structural model constructed by Haumann et al. [25] based on EXAFS data, a five-coordinate

Mn(III) in the S_2 state was proposed, which can therefore be a Mn(III) ion with $^5B_1$ symmetry. This is particularly pertinent given the EPR studies mentioned above.

The next question is then which of the Mn ions in the $CaMn_4$ cluster fulfils the above criteria for the methanol-binding Mn ion. The identity for this ion can be narrowed down by examining available FT-IR spectroscopic data. Kimura et al. [40] have showed by difference FT-IR spectroscopy that ^{2}Mn is oxidised from Mn(III) to Mn(IV) during the $S_1 \rightarrow S_2$ transition. This rules out ^{2}Mn as the binding Mn ion, in agreement with its lack of methanol accessibility according to the solvent contact, surfaces here. Difference FT-IR spectroscopy was also employed by Debus et al. [41] to demonstrate that ^{4}Mn does not undergo oxidation in any S-state transition. In combination with the simulation of the methanol form of the S_2 multiline by Peloquin et al. [33], ^{4}Mn would remain as Mn(IV) in all S-states.[1] Therefore, only ^{1}Mn or ^{3}Mn could be a Mn(III) ion in the S_2 state, and thus candidates for the methanol binding Mn ion.

We can then turn to our solvent accessibility analysis to decide which of ^{1}Mn and ^{3}Mn would more likely be the methanol binding Mn ion. From Fig. 1, it can be seen that methanol has much better access to ^{3}Mn than ^{1}Mn, with a tighter ligand environment around the latter hindering close approach of methanol. Therefore, while one should be careful to bear in mind that the calculated solvent contact surfaces are based on a medium-resolution crystal structure, the currently available data suggest that ^{3}Mn is more likely to be the ion to which methanol binds.

3.3. Electrostatic considerations

Apart from the spatial considerations examined by the solvent contact surfaces, a channel involved in methanol access should also be reasonable from an electrostatic/hydrophilicity point of view.

Examining the residues that are involved in forming the narrow and broad channels, the majority of residues forming the walls of these accessibility channels had potential hydrogen bond acceptor atoms (O or N) making contact with the channel, with nearly half of these atoms coming from amino acid side chains rather than the protein backbone (Supplementary materials Table A). It is therefore reasonable to suggest that the channels have good potential for conducting polar solvent molecules.

The same analysis for the residues that are involved in forming the back channel (Supplementary materials Table B) showed that again a large majority of residues have at least one potential hydrogen bond acceptor pointing towards the channel. In particular, at the top of the back channel closest to the Ca ion of the $CaMn_4$ cluster, the residues D1-Tyr 161, -Gln 165, -His 190 and -Asn 296 form a tight network of N and O atoms just where a gap separates the back and broad channels (Fig. 2C). These closely spaced groups could potentially take part in hydrogen bonding with solvent molecules. Therefore, the back channel can also be regarded as potentially suitable for the passage of polar solvent molecules.

3.4. Extent of the access channels

When the solvent accessibility calculation was extended beyond the initial search volume and out towards the protein surface, the back channel identified above was found to be continuous and open all the way to the lumen (Fig. 2D), with the residues D1-Ala 88, -Ile 89, -His 92, -Tyr 94, CP43-Pro 345, -Thr 346, and -Trp 359 forming the exit. This makes it a clear candidate for a channel capable of allowing methanol access from the lumen to the $CaMn_4$ cluster. However, this back channel does not reach any of the Mn ions in the cluster. By contrast, while the narrow and broad channels do make contact with the Mn (and Ca) ions in the cluster, as well as point outwards towards the lumen, they were found not to be open all the way to the luminal surface. The broader channel was found to close at a distance of ~12 Å away from the $CaMn_4$ cluster, whereas the narrower channel extended slightly further, to a distance of ~16 Å from the cluster.

A possible interpretation is that the narrow and broad channels were merely free space in the protein rather than access channels. However, their length and continuous nature suggest otherwise, especially in comparison to the much smaller sizes of the numerous other isolated pockets of free space in the protein. Rather, it should be noted that the crystal structure is a static model of the protein. Hence it may be possible that dynamic thermal motion ("breathing") of the protein permits continued solvent access towards the lumen [42,43]. This effect would become increasingly significant moving away from the $CaMn_4$ cluster, as the protein environment becomes less restricted by the numerous ligations to the cluster. Therefore, this could be one mechanism by which solvent could enter the narrow and wide channels under physiological conditions.

Having regard to the complementary characteristics of the back channel opening out to the lumen but not reaching the Mn ions, and vice versa for the narrow and broad channels, another possibility is that narrow and broad channels remain closed to methanol even under physiological conditions, but dynamic thermal motion leads to transient widening of the gap between the two channels (Fig. 2B). Methanol can then enter from the lumen, down the back channel, and cross over to the broad channel, which would then provide an access route to the $CaMn_4$ cluster, all the way from the luminal surface. A further variant of this, involving a more active gating mechanism at the gap, is discussed in detail in the context of water accessibility below.

3.5. Water accessible surface

To investigate water accessibility through PSII, solvent contact surfaces were calculated with a probe radius appropriate for water (1.4 Å). While the methanol channels identified above all had similar, and slightly wider analogues in the water contact surface, there were also many interesting differences in terms of extra branches and new exit pathways to the lumen. These are

[1] This model is also compatible with both the ligand- and Mn-oxidation models for the $S_2 \rightarrow S_3$ transition, as at least one Mn ion is in the 4+ state throughout the S-cycle in both, whereas there would be no Mn(III) present in the S_3 state in the Mn-oxidation model.

first described in turn below and compared with the access channels very recently calculated by Murray and Barber [12] using a similar method. This is followed by discussions about the possible functions of these channels.

3.5.1. Back channel

The back channel showed the highest degree of similarity between the water and methanol surfaces, and it remained open to the lumen. The gap between the back and broad channels also remained, surrounded by the same residues as for the methanol access surface. The size of the gap was however smaller, as expected, given the smaller sized probe used for calculating water accessibility. This back channel corresponded to channel (i) in the study by Murray and Barber [12]. All but four of the residues (D1-His 332, -Glu 333, CP43-Gly 220, -Glu 354) which Murray and Barber have assigned to channel (i) were also found to be involved in the formation of the back channel (Table 1 and Supplementary materials Table B). Otherwise, the differences observed between these two studies lie mainly in where the channel was regarded to end at the extremities, and that some walls of the channel (i) were not clearly defined in the results by Murray and Barber (Supplementary materials Fig. A). In our study, we have identified further residues which complete the formation of this channel, closing off all the walls. Without these extra residues, certain sides of the channel are open (Supplementary materials Fig. A). Overall, however, the results of these two studies concur with respect to the existence of this channel.

3.5.2. Narrow and broad channels

The narrow and broad channels found in the methanol surface were also present in the solvent contact surface for water (Fig. 3), though with two particularly important differences.

Firstly, it was found that ^{1}Mn could also be accessed when the water-sized probe was used (Fig. 3A). This extra "lobe" of access is shared by both ^{1}Mn and ^{3}Mn. Hence, ^{1}Mn would be accessible to water, even though methanol would not be able to approach close enough to bind.

Secondly, while the broad channel remained closed in the water contact surface, a new side branch was found to radiate from the narrow channel (dotted oval in Fig. 3B). When this side branch was followed, it was found to be open and continuous all the way to the lumen (Fig. 3C), exiting at the residues CP47-Arg 385, -Ala 386, -Ser 388, PsbU-Leu 47, -Tyr 51, -Leu 121, -Asp 126 and -Asn 130. This is in stark contrast to the methanol surface where both the narrow and brood channels were closed to lumen access (see above). The additional residues forming this extension are listed in Supplementary materials Table C. Thus, the narrow channel represents an addition, open channel leading from the $CaMn_4$ cluster to the lumen side in the water contact surface.

This extended narrow channel was not reported in the study by Murray and Barber [12]. To check whether this difference was due to the use of different crystal structures in the two studies (PDB ID 2AXT here, 1S5L in Murray and Barber), we calculated and analysed the water solvent contact surface for the 1S5L structure also. A corresponding open channel formed by the same residues was found also in the 1S5L structure using our method of calculation, with some minor differences in the shape and diameter for the channel, deriving from differences in orientations of the relevant residues in the two structures (Fig. 3D).

Another difference between the channels found in the two studies is that we found no correspondence to channel (iii) in the Murray and Barber study [12]. When this was examined more closely, it was discovered that our broad channel overlapped with the proximal end of channel (iii). Beyond this, however, we found instead that channel (iii) was blocked for passage of water by four residues (D1-Glu 65, -Pro 66, -Val 67, D2-Glu 312) about halfway along its path (Supplementary materials Fig. B). This blockage was present even when the 1S5L structure was used for calculations. A channel extending from this blockage to the lumen was observed, but we found no continuously open channel from the $CaMn_4$ cluster leading to the lumen formed by the residues assigned to channel (iii). In this sense, channel (iii) can be seen as a blocked extension of the broad channel identified in this study.

3.5.3. Large channel system

In addition to the channels we have identified so far, an additional, large system was found for the water solvent contact surface. This consisted of three connected and continuously open channels leading from the $CaMn_4$ cluster to the lumen (Fig. 4A). The residues lining the walls of this system within the initial search radius of 15 Å are listed in Table 1. A more complete and detailed list of the remaining residues is presented in Supplementary materials Table D. While much of the large spaces within this system were also present in the methanol surface, there was no open connection to the $CaMn_4$ cluster there. By contrast, in the solvent contact surface for water, this channel system was found to be connected to the back channel/channel (i) [12], near the Ca^{2+} ion of the $CaMn_4$ cluster (see below).

A comparison with the results by Murray and Barber showed that this system included the residues forming the channel denoted channel (ii) by these authors (Fig. 4 and Supplementary materials Table D). Only one exit to this channel was explicitly mentioned in that study [12], near PsbV-Tyr 136, -Tyr 137 and PsbU-Lys 134, which we also found (dashed arrow in Fig. 4A). However, we also found a large opening to the lumen at the distal end of channel (ii) (PsbV-Gln 60, CP43-Lys 79, -Glu 83, -His 398, -Val 417, -Asn 418, -Phe 419; solid arrow in Fig. 4A). After including additional residues to completely describe the fully enclosed channels (at which point it could be seen that PsbV-Ser 65 is also part of this latter opening), it was found that these two exits can be regarded to derive from two separate channels that share a common proximal end at the $CaMn_4$ cluster (Fig. 4). In addition, a third, much broader channel was found in the channel system, positioned between the other two, again sharing a common proximal end with the other two channels (Fig. 4A). This third channel led to two other exits to the lumen, one at CP43-Asn 415, -Ser 416, PsbJ-Ser 39, -Leu 40 and PsbV-Gln 60, and the other at D1-Ile 307, -Gly 311, PsbJ-Leu 40, PsbV-Tyr 52, -Lys 56, and -Ile 151 (dotted arrows in Fig. 4A). Overall, then, starting from being one channel at the end proximal to the $CaMn_4$ cluster, this large channel system

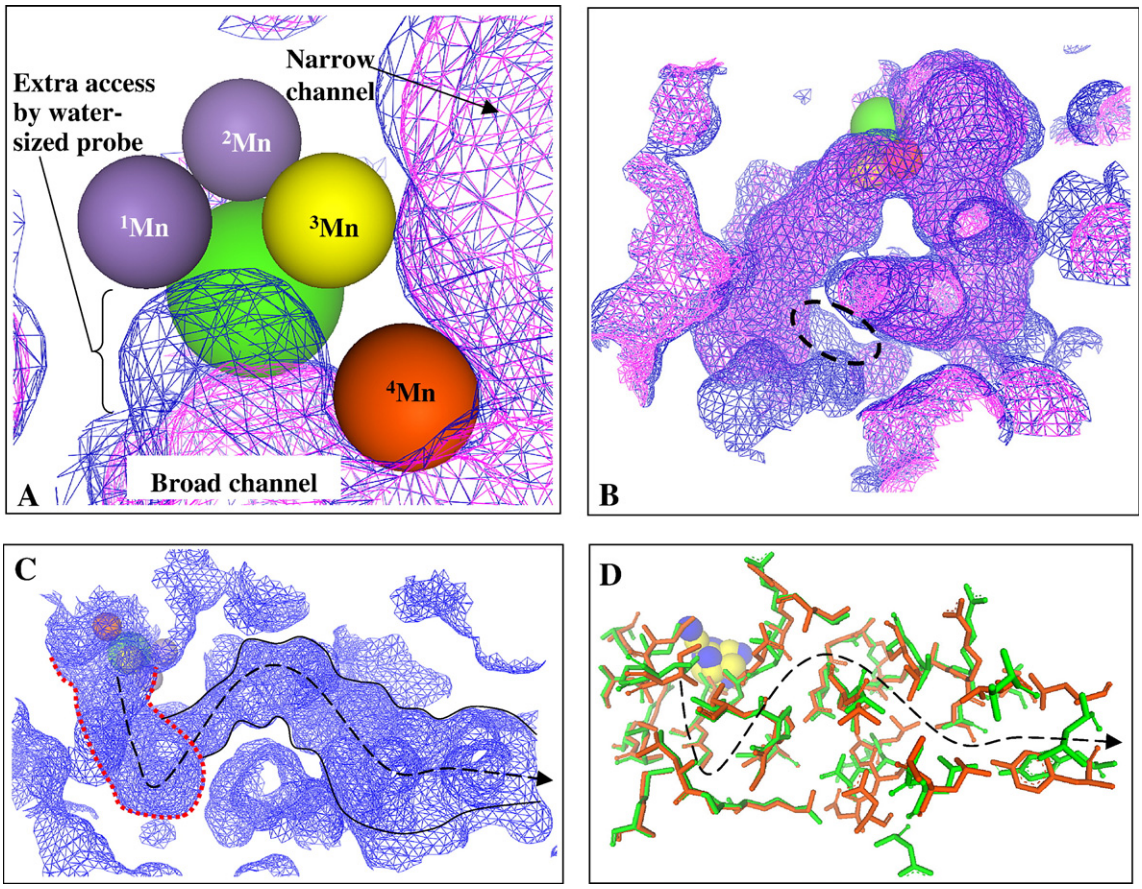

Fig. 3. Characteristics of the extended narrow channel in the water solvent contact surface. The residues forming this extension are listed in Supplementary materials Table C. (A) Comparison of methanol (pink) and water (blue) contact surfaces at the $CaMn_4$ cluster, generated using probe radii of 1.7 Å and 1.4 Å, respectively. An extra access lobe is found in the water contact surface, giving access to both ^{1}Mn and ^{3}Mn, while ^{1}Mn is not accessible in the methanol contact surface. The lobe is situated near the juncture between the narrow and broad channels, where ^{4}Mn is positioned as marked. (B) Superposition of the narrow and broad channels in the methanol (pink) and water (blue) contact surfaces. The dashed oval marks the extra branch radiating from the narrow channel in the water contact surface. (C) The extended narrow channel in the water contact surface (outlined with solid lines). The region corresponding to the (closed) narrow channel in the methanol contact surface is outlined with a red dotted line. The path of the channel leading out to the lumen is marked with the dashed arrow. (D) RMS best fit superimposition of the residues involved in forming the extended narrow channel from the Loll et al. (orange [11]) and the Ferreira et al. (green [13]) crystal structures (PDB ID 2AXT and 1S5L, respectively). The $CaMn_4$ cluster from the Loll et al. structure is coloured blue, and that from the Ferreira et al. structure is coloured yellow. The viewing angle is the same as for panel C. The path of the back channel is marked with the dashed arrow.

splits up into three channels leading to four exits towards the lumen (Fig. 4A). An interesting observation is that the branches which make up this channel system run along the surface of the extrinsic subunit PsbV, radiating out from the $CaMn_4$ cluster, reminiscent of ski slopes on a hill (Fig. 4B).

3.6. Summary of the water accessibility channels

The relative position of the water accessible channels identified, as well as their location within the PSII protein, is summarised in Fig. 5A and B. It can be seen that all the channels exit below the membrane plane on the luminal side (Fig. 5A). However, the back channel/channel (i) and the large channel system are directed to a direction opposite to that of the narrow channel and the broad channel/channel (iii). Furthermore, it can be seen that the back channel is connected to the large channel system near the $CaMn_4$ cluster (Fig. 5B). Our calculations have thus identified three sets of (open) channels which could serve as pathways for the entry of water, and exit of H^+ and O_2.

The differences observed between this study and that of Murray and Barber [12] are likely to lie in the different simulation methods employed. Whereas an automated search was used in Murray and Barber to identify open pathways between the position of the $CaMn_4$ cluster and the outer convex hull of PSII, we calculated all possible solvent accessible regions around the catalytic centre, regardless of whether they were connected to the exterior of the protein. The full solvent contact surfaces were then examined in detail to locate the channels (see Materials and methods). It is unclear why some open channels we identified here were not reported by Murray and Barber, at the same time that they observe the broad channel opening out to the lumen, which we do not. It may be that the automatic search algorithm led to these features to be missed.

Our identification of extra residues that were involved in the building of the channels was again based on direct inspection of all the residues near the walls of the channels to see which ones made contact with the channels. By contrast, Murray and Barber defined the residues involved in the channels' formation as those

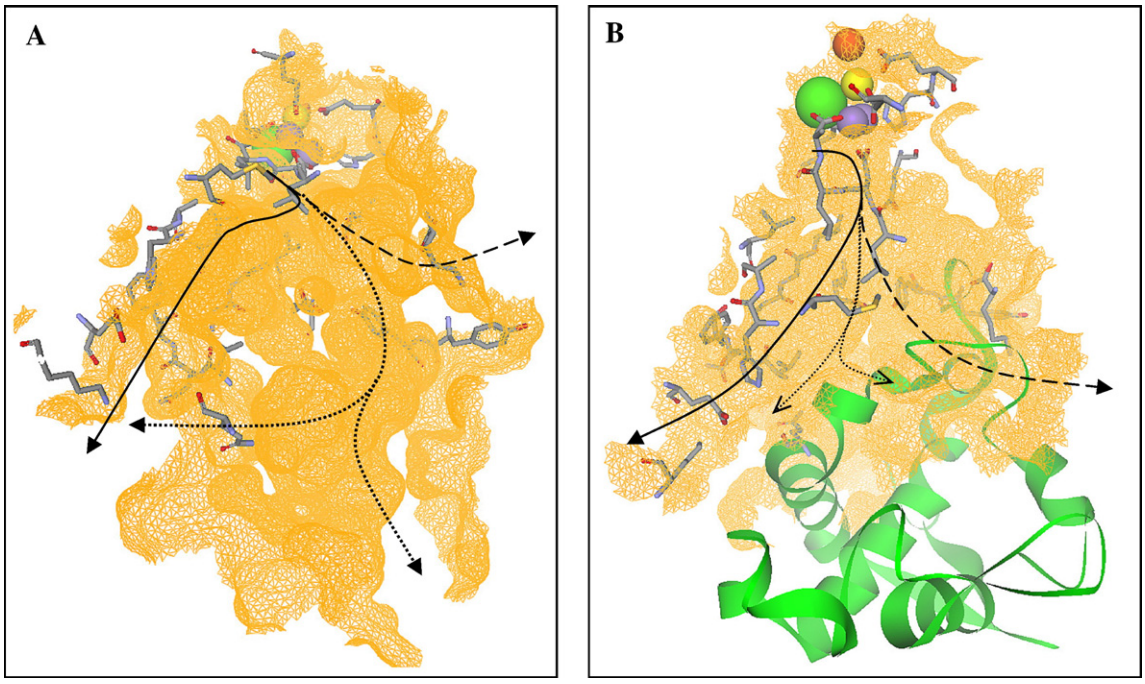

Fig. 4. The large extra channel system in the water contact surface leading from the $CaMn_4$ to the luminal side of PSII. The residues lining this channel system are listed in Table 1 and Supplementary materials Table D. (A) The pathways of the branches of the channel system are marked by the solid, dashed and dotted arrows. The residues identified as involved in channel (ii) in Murray and Barber are shown in stick representation. These residues are involved in two branches in the channel system (solid and dashed lines). The two exits from the large central branch are shown with the split dotted arrow. The $CaMn_4$ is shown in space-filling representation. A front clipping plane was applied to enhance clarity. (B) A rotated view of the channel system, showing in addition the position of the subunit PsbV (green ribbon). The two branches marked by the solid and dashed arrows in panel A run in opposite directions across the top of the PsbV subunit. The large central branched extends behind the PsbV subunit (dotted arrow).

within 4 Å of the centre of the channel pathway [12]. This may explain why certain residues were not included as being involved with the channels, especially where the channels are wide.

Finally, as the $CaMn_4$ cluster was removed before calculations were initiated in Murray and Barber [12], details of exactly where solvent molecules can make contact with the Ca^{2+} and Mn ions are lost. In particularly, the gap between the back and broad channels would have been missed, as Ca^{2+} is part of the ensemble which gives rise to the gap in solvent accessibility (see above).

3.7. Function of the water accessible channels: H^+ exit channel

The release of H^+ after water oxidation is likely to occur via specific routes within the protein to direct it towards the lumen to contribute to the maintenance of the transmembrane H^+ gradient. Leakage of protons to the stroma needs to be avoided. It is therefore reasonable that there would be an H^+ exit channel to facilitate this. As has been observed with other enzymes such as cytochrome *c* oxidase and bacteriorhodopsin, H^+ movement can be achieved via a channel of water molecules (such as via the Grotthus mechanism), possibly involving also amino acid residues that donate and accept protons. Therefore, in identifying putative water channels in PSII, possible H^+ channels can also be assigned. We propose here that the extended narrow channel (Figs. 3C and 5) corresponds to such a channel, which can direct H^+ away from the $CaMn_4$ cluster after water oxidation.

Potential water/H^+ channels in PSII have been proposed by Barber and co-workers [13,44] and by Ishikita et al. [45], based on examinations of the polarity of the residues leading away from the $CaMn_4$ cluster, and calculated changes in pK_a values during S-state transitions. In Fig. 5C, the residues belonging to the D1, D2 and CP43-subunits studied by Ishikita et al. [45] and Barber and co-workers [13,44] are superimposed onto the access channels identified in this study. Many of the electrostatically relevant residues were in the vicinity of the narrow and broad channels in the water solvent contact surface. In particular, all four residues which were found by Ishikita et al. [45] to undergo large shifts in calculated pK_a values between the S_0 and S_4 states (D1-Asp 59, -Asp 61, CP43-Arg 357, D2-Lys 317) are in contact with the narrow and broad channels, as were all four residues proposed by Barber and co-workers to form the beginning of the proton/water channel (D1-Asp 61, -Glu65, D2-Glu 312, -K317). These residues are highlighted in Fig. 5C, showing their participation in the formation of the narrow and broad channels. Both channels are hydrophilic in nature (Supplementary materials Tables A and C), and the narrow channel extends all the way to the luminal side. Therefore, we propose that the broad and narrow channels function together as a H^+ exit channel. The relatively narrow nature of this channel is consistent with the potential presence of an ordered network of water molecules which could facilitate the movement of H^+ down the channel, possibly with the participation of amino acid residues lining the channel. Furthermore, this assignment agrees well with various proposals for the mechanism of water

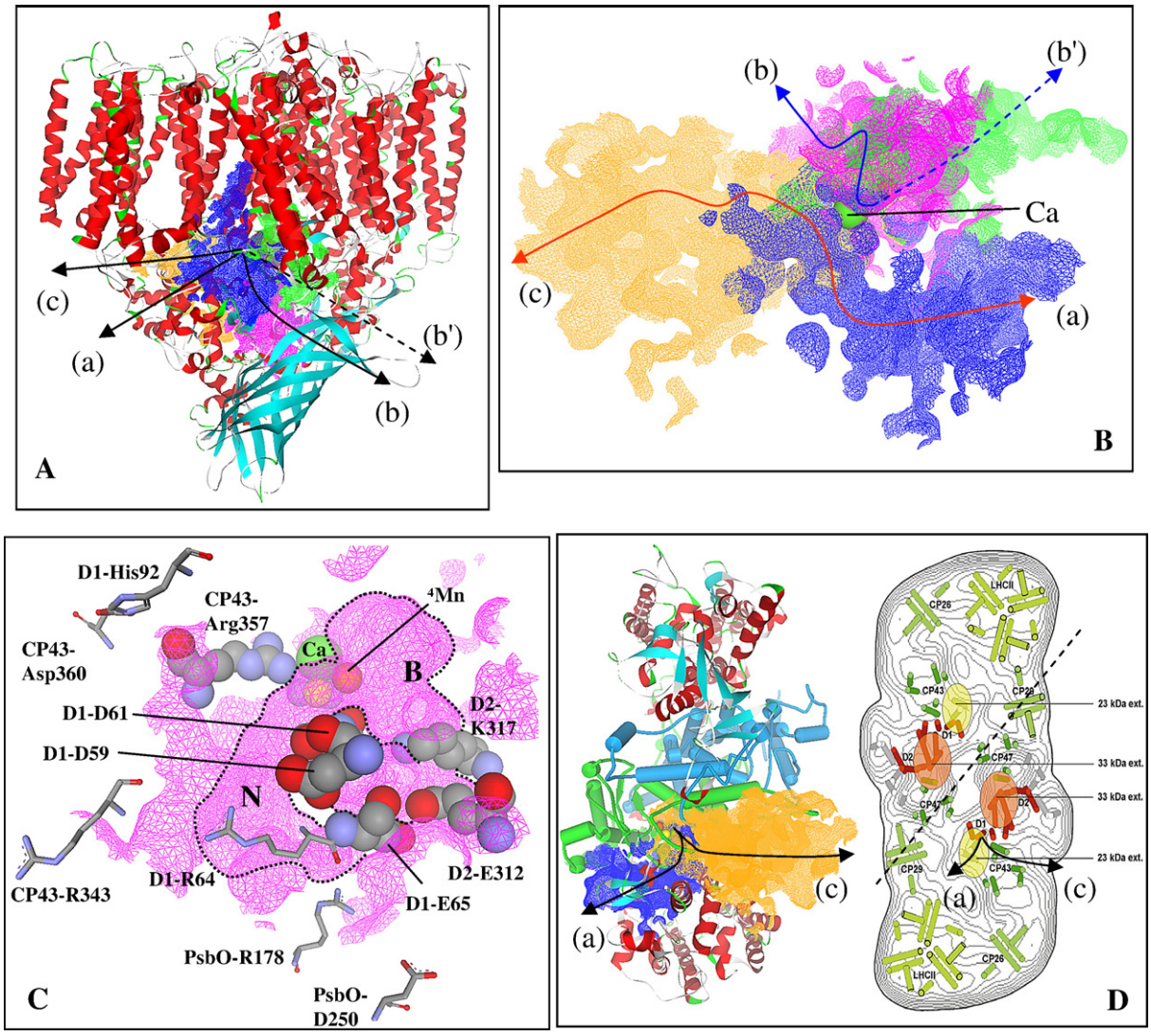

Fig. 5. Further characterisation of the water accessible channels. (A) The path of the (a) back channel/channel (i), (b) extended narrow channel, (b′) channel (iii) in Murray and Barber [12], and (c) large channel system are shown, relative to the PSII protein, viewed along the membrane plane. (B) Paths of the same channels, viewed normal to the membrane plane from the stromal side. The connection between the back channel/channel (i) and the large channel system are shown with the red double arrow (for clarity, only the large central branch of the large channel system is marked here). The extended narrow channel and channel (iii) are also connected, shown by the blue double arrow (channel (iii) is shown with a dashed arrow, as it was not found to be continuously open in our calculations). The gap between the two channel systems occurs at the Ca^{2+} ion of the $CaMn_4$ cluster, as marked. (C) Residues proposed by Ishikita et al. [45] and Barber and co-workers [13,44] as part of water and/or H^+ channels are superimposed on the narrow ("N") and broad ("B") channels (dashed outline) of the water contact surface (cf., Fig. 3B). The residues highlighted with space-filling representation are those indicated by Ishikita et al. [45] as showing a large calculated shift in pK_a values between the S_0 and S_4 states and those by Barber and co-workers [13,44] as being involved in a proton/water channel that also makes contact with the solvent accessible channels. The Ca^{2+} and ^{4}Mn ions of the $CaMn_4$ cluster are marked. (D) On the left, the directions of the back channel/channel (i) [arrow (a)] and the large channel system [arrow (c)] are shown, relative to the D1 (green), D2 (blue), and the CP43 and CP47 protein subunits (ribbons), and viewed down the membrane normal from the luminal side. On the right, this is compared with the organisation of the PSII supercomplex, including the light harvesting subunits CP26, CP29, and LHCII, as determined by cryogenic electron microscopy (reproduced with permission from Barber et al. [48]).

oxidation which favour the binding of substrate water molecules to ^{4}Mn and Ca [4,13,23,46]. The final step generating molecular O_2 and H^+ would then occur in the vicinity of ^{4}Mn, which is at the cusp of the narrow and broad channels, opposite the D1–D61 residue. The H^+ released can then be conducted down the narrow channel towards the lumen. Significantly, the recent QM/MM study by Sproviero et al. [23] found two hydrogen-bonded water molecules between ^{4}Mn and D1-D61, which the authors also suggested to constitute the beginning of a H^+ exit channel.

A proposal for a water/H^+ channel was also presented by Murray and Barber in their recent channel calculations [12]. However, the authors favoured channel (iii) as the water/H^+ channel, which corresponds approximately to an extended broad channel. As stated above, we do not find a continuously open channel corresponding to channel (iii). Moreover, in contrast to channel (iii) as identified by Murray and Barber, our assignment additionally incorporates CP43-Arg 357 as part of the H^+ channel. This residue was found to give the greatest calculated pK_a shift in the $S_4 \rightarrow S_0$ transition (−1.7 to 15.5) [45],

and was also identified by QM/MM calculations as an important residue in a proposed H^+ abstraction mechanism [23].

3.8. Function of the water accessible channels: water entry and O_2 exit channels

The remaining two channels, the back channel/channel (i) and the extra channel system (incorporating channel (ii) in Murray and Barber) could therefore function as channels for the transport of substrate water to the $CaMn_4$ cluster and for the exit of O_2 formed from water oxidation. Anderson [47] has suggested the existence of a O_2 channel in PSII to rapidly direct molecular oxygen away from PSII, and in particular P680, in order to avoid the formation of the highly oxidising singlet oxygen through reaction with triplet chlorophyll generated from photoexcited chlorophyll molecules. While oxidative damage by singlet oxygen would be particularly harmful near P680, it is desirable to avoid singlet oxygen formation throughout PSII.

Murray and Barber assigned the back channel/channel (i) to such an oxygen removal function, on the basis that it was the least hydrophilic of the three channels observed in their study, and by analogy to their analysis of cytochrome *c* oxidase. Their channel (ii) was then assigned as an alternate water/H^+ channel. While this is a possible interpretation, we propose instead that these two connected channels should be considered together (Fig. 5B), where both branches could supply substrate water to the $CaMn_4$ cluster, as well as allow the exit of molecular O_2.

Nevertheless, several factors do suggest that the extra channel system that we observe in the water contact surface could be the preferred O_2 exit route. The first is based on the geometry of the channel system. Starting from being one channel at the end proximal to the $CaMn_4$ cluster, the system spreads out into three channels leading to four exits towards the lumen, with the middle channel being particularly broad (Fig. 4A). Given that O_2 should be removed as soon as possible, the large size and availability of multiple channels and exits of this system make it a better candidate for O_2 removal than the back channel/channel (i), which is by contrast a channel with only one exit. A second factor is the position of the exits to the lumen. Fig. 5D compares the relative positions of the back channel/channel (i) and the large channel system with the positions of the various subunits in a PSII supercomplex as identified by cryogenic electron microscopy [48]. It can be seen that while the exits of the large channel system point out away from the supercomplex, the exit of the back channel/channel (i) points towards the chlorophyll-rich CP29 and LHCII assemblies. Although the channels exit beneath the membrane plane and do not point directly into the intra-membrane space, it is arguably still desirable to direct molecular O_2 away from the chlorophyll molecules contained within these assemblies, where triplet chlorophyll formation could frequently occur.

An interesting observation from the literature is that the removal of PsbV, either biochemically or genetically, has a relatively minimal effect on the ability of PSII to evolve oxygen under mild environmental conditions (reviewed in [22]). This may be consistent with the close association of the large channel system with PsbV. While it facilitates vectorial removal of O_2 away from the $CaMn_4$ cluster, this role is probably more or less passive, given the apolar nature of molecular oxygen. Hence it is reasonable that removal of PsbV and thus the large channel system only has minor deleterious effects. If the channels were instead associated with substrate water access or H^+ exit, their removal would be expected to cause more significant damage to PSII function. This is especially true for H^+ exit, which is likely to require a protein channel to provide a chain of water and possibly key amino acids residues to allow directed transport through the protein.

We do not claim that the above assignment is definitive. Given that the back channel/channel (i) and the large channel system are connected, the substrate water access and O_2 exit functions need not be mutually exclusive. Indeed both sets of channels are expected to be replete with water molecules and could supply the $CaMn_4$ cluster with substrate. It is however interesting to further note that the residues which Ishikita et al. [45] identified electrostatically as involved in a possible "alternate" water channel (D1-His 92, CP43-Arg 353, -Glu 360) are part of the back channel/channel (i) (Supplementary materials Table B).

3.9. Proposed control gate mechanism for water access to the $CaMn_4$ cluster

Given the functional assignments of the channels presented above, the question arises as to how substrate water flowing in from the back channel can reach the necessary Mn ion(s) to allow their binding for water oxidation, given that this channel only makes contact with Ca^{2+}, and not the rest of the $CaMn_4$ cluster. As mentioned above, it may be possible that ordinary thermal motion could lead to transient widening of the opening at the gap between the back and broad channels to allow cross over from the back channel to the broad channel [42,43]. However, given that random thermal motion of the residues near the $CaMn_4$ cluster is likely to be rather more restricted due to the number of residues ligating to the cluster, passage across the gap could involve a more active process. One such alternative mechanism could be related to the S-state-dependent changes in the structure of the $CaMn_4$ cluster, as demonstrated by EXAFS spectroscopy [25,26]. These structural changes could bring about shifts in the positions of the amino acid residues around the cluster, including the mechanistically significant residues surrounding the gap (see above), as well as alterations in putative hydrogen-bonding networks between nearby residues (see, e.g., Fig. 2C). Such movements may lead to an increase in the diameter of the opening in an S-state-dependent manner, allowing water to cross over from the back to the broad channel and thus access the Mn ions. Such a gap-crossing mechanism could then act as a "control gate" to regulate the flow of water to the $CaMn_4$ cluster during water oxidation.

The existence of some mechanism for controlling water access to the $CaMn_4$ cluster has previously been suggested [49–56]. One potential reason for having such a gating mechanism is the prevention of unwanted side reactions due to excess number of water molecules at or near the $CaMn_4$ cluster [50,54,55]. Another reason suggested for controlling water access is to

ensure optimal binding conformation(s) required for water oxidation [55,56], at specific binding sites [57,58].

Experimentally, the importance of the Ca^{2+} ion in controlling ligand access and binding to Mn ions in the $CaMn_4$ cluster has been demonstrated. Ca-depletion leads to increased access to the Mn ions by large molecules [52,54], and gives rise to an unusually stable and modified S_2-state multiline EPR signal [50,52,59]. It has also been shown that Mn ions in the $CaMn_4$ cluster are protected from extrinsic electron donors by the presence of the Ca^{2+} ion [53,54]. The experimentally observed importance of the Ca^{2+} ion finds direct correspondence to our present simulations, where Ca^{2+} is part of the ensemble that forms the gap between the back and broad channels (Fig. 2).

Two further points should be noted here. Firstly, regardless of the actual mechanism that allows solvent molecules to access the Mn ions, and whether or not the control gate mechanism exists, the conclusions above regarding the identity of the methanol-binding Mn ion are not affected. These were based on methanol accessibility at the cluster itself rather than how the methanol arrived in the first place. Secondly, the solvent contact surfaces suggest that it is unlikely that Y_Z exists in a hydrophobic environment, as argued by Zhang [60]. Based on our solvent accessibility calculations, Y_Z makes direct contact with the back channel that is open for water access all the way out to the lumen. It is also in contact with the broad channel, which is connected to the extended narrow channel. The latter is again accessible to water from the luminal side. Thus, the hydrophilic environment around Y_Z that was pointed out in early modelling work [61,62] is now confirmed by the crystal structure and our solvent accessibility analysis.

4. Conclusions

By analysing solvent access channels and considering the available spectroscopic data on methanol effects, we have concluded that ^{3}Mn is the most likely candidate for the binding of methanol. Furthermore, examination of the solvent contact surfaces for water has pointed to the existence of several channels which could act as conduits for the entry of substrate water and the exit of product O_2 and H^+. The identification of these features within the PSII structure opens up the possibility of further mutation studies in sites more distant from the $CaMn_4$ cluster, directed at elucidating the mechanism of transport and binding of methanol and water.

This study has concerned itself with an examination of the static crystal structure of PSII. Clearly there is still much room for further investigations. In the context of assigning functions to the channels, important factors such as the channels' hydrophilicity/hydrophobicity, amino acid participation, structural/steric characteristics, and existence of hydrogen-bonding networks can be analysed in more detail that has been possible in the present study. In particular, techniques such as molecular dynamics (MD) simulations with explicit water molecules and site-directed mutagenesis would be very useful in this regard. These approaches have played a key part in elucidating the role of these factors in the water and proton transport processes in aquaporin and cytochrome *c* oxidase [63–67], and should also be most enlightening in studying PSII. It is likely that these channel studies can also be extended to the investigation of effects caused by the addition of other small molecules, and also provoke interesting studies involving the application of mutagenesis to regions in PSII not earlier recognised as "hot spots" for such experiments.

Acknowledgements

The authors would like to thank Dr. Fikret Mamedov, Dr. Anders Thapper and Kajsa Havelius for their helpful discussions.

The financial support from the Swedish Research Council, the European Community Sixth Framework Programme Marie Curie Incoming International Fellowship (514817 to F.M.H.), and the Swedish Energy Agency is gratefully acknowledged.

Appendix A. Supplementary data

Supplementary data associated with this article can be found, in the online version, at doi:10.1016/j.bbabio.2007.08.009.

References

[1] G. Renger, Photosynthetic water oxidation to molecular oxygen: apparatus and mechanism, Biochim. Biophys. Acta 1503 (2001) 210–228.
[2] C. Goussias, A. Boussac, A.W. Rutherford, Photosystem II and photosynthetic oxidation of water: an overview, Philos. Trans. R. Soc. Lond., B Biol. Sci. 357 (2002) 1369–1381.
[3] T.J. Wydrzynski, K. Satoh (Eds.), Photosystem II: The Light-driven Water: Plastoquinone Oxidoreductase, Springer, The Netherlands, 2005.
[4] J.P. McEvoy, G.W. Brudvig, Water-splitting chemistry of Photosystem II, Chem. Rev. 106 (2006) 4455–4483.
[5] J. Nugent (Ed.), Special Issue: Photosynthetic Water Oxidation, Biochim. Biophys. Acta, vol. 1503, 2001, pp. 1–259.
[6] C. Tommos, P. Brzezinski, A. Ehrenberg (Eds.), Special issue dedicated to Jerry Babcock, Biochim. Biophys. Acta, vol. 1655, 2004, pp. 1–413.
[7] J. Messinger, W. Lubitz (Eds.), Special Issue: Biophysical Studies on Photosystem II and Related Model Systems, Phys. Chem. Chem. Phys., vol. 6, 2004, pp. 4733–4911.
[8] J. Nield, P.J. Nixon (Eds.), Special Issue Dedicated to James Barber, Photochem. Photbiol. Sci., vol. 4, 2005, pp. 916–1096.
[9] S.I. Allakhverdiev, E.M. Aro, V.V. Klimov, T. Nagata, K. Satoh, V.A. Shuvalov, A. Telfer, T. Wydrzynski (Eds.), Special Issue: Structure and Function of Photosystems, Biochim. Biophys. Acta, vol. 1767, 2007, pp. 401–882.
[10] J.H. Su, K.G.V. Havelius, F. Mamedov, F.M. Ho, S. Styring, Split EPR signals from Photosystem II are modified by methanol, reflecting S state-dependent binding and alterations in the magnetic coupling in the $CaMn_4$ cluster, Biochemistry 45 (2006) 7617–7627.
[11] B. Loll, J. Kern, W. Saenger, A. Zouni, J. Biesiadka, Towards complete cofactor arrangement in the 3.0 angstrom resolution structure of Photosystem II, Nature 438 (2005) 1040–1044.
[12] J.W. Murray, J. Barber, Structural characteristics of channels and pathways in Photosystem II including the identification of an oxygen channel, J. Struct. Biol. 159 (2007) 228–237.
[13] K.N. Ferreira, T.M. Iverson, K. Maghlaoui, J. Barber, S. Iwata, Architecture of the photosynthetic oxygen-evolving center, Science 303 (2004) 1831–1838.
[14] H. Kovacs, A.E. Mark, J. Johansson, W.F. van Gunsteren, The effect of

environment on the stability of an integral membrane helix-molecular-dynamics simulations of surfactant protein-C in chloroform, methanol and water, J. Mol. Biol. 247 (1995) 808–822.
[15] J. Norberg, L. Nilsson, Solvent influence on base stacking, Biophys. J. 74 (1998) 394–402.
[16] D.A. Force, D.W. Randall, G.A. Lorigan, K.L. Clemens, R.D. Britt, ESEEM studies of alcohol binding to the manganese cluster of the oxygen evolving complex of Photosystem II, J. Am. Chem. Soc. 120 (1998) 13321–13333.
[17] K.A. Åhrling, M.C.W. Evans, J.H.A. Nugent, R.J. Ball, R.J. Pace, ESEEM studies of substrate water and small alcohol binding to the oxygen-evolving complex of Photosystem II during functional turnover, Biochemistry 45 (2006) 7069–7082.
[18] G. Bernát, F. Morvaridi, Y. Feyziyev, S. Styring, pH dependence of the four individual transitions in the catalytic S-cycle during photosynthetic oxygen evolution, Biochemistry 41 (2002) 5830–5843.
[19] T. Tsukihara, H. Aoyama, E. Yamashita, T. Tomizaki, H. Yamaguchi, K. ShinzawaItoh, R. Nakashima, R. Yaono, S. Yoshikawa, The whole structure of the 13-subunit oxidized cytochrome *c* oxidase at 2.8 angstrom, Science 272 (1996) 1136–1144.
[20] T. Tsukihara, K. Shimokata, Y. Katayama, H. Shimada, K. Muramoto, H. Aoyoma, M. Mochizuki, K. Shinzawa-Itoh, E. Yamashita, M. Yao, Y. Ishimura, S. Yoshikawa, The low-spin heme of cytochrome *c* oxidase as the driving element of the proton-pumping process, Proc. Natl. Acad. Sci. U. S. A. 100 (2003) 15304–15309.
[21] C. Tommos, Electron, proton and hydrogen-atom transfers in photosynthetic water oxidation, Philos. Trans. R. Soc. Lond., B Biol. Sci. 357 (2002) 1383–1394.
[22] R.J. Debus, The catalytic manganese cluster: protein ligation, in: T. Wydrzynski, K. Satoh (Eds.), Photosystem II: The Light-driven Water: Plastoquinone Oxidoreductase, Springer, The Netherlands, 2005, pp. 261–284.
[23] E.M. Sproviero, J.A. Gascon, J.P. McEvoy, G.W. Brudvig, V.S. Batista, Quantum mechanics/molecular mechanics structural models of the oxygen-evolving complex of Photosystem II, Curr. Opin. Struct. Biol. 17 (2007) 173–180.
[24] Z. Deák, S. Peterson, P. Geijer, K.A. Åhrling, S. Styring, Methanol modification of the electron paramagnetic resonance signals from the S_0 and S_2 states of the water-oxidizing complex of Photosystem II, Biochim. Biophys. Acta 1412 (1999) 240–249.
[25] M. Haumann, C. Muller, P. Liebisch, L. Iuzzolino, J. Dittmer, M. Grabolle, T. Neisius, W. Meyer-Klaucke, H. Dau, Structural and oxidation state changes of the Photosystem II manganese complex in four transitions of the water oxidation cycle ($S_0 \rightarrow S_1$, $S_1 \rightarrow S_2$, $S_2 \rightarrow S_3$, and $S_3 \rightarrow S_4 \rightarrow S_0$) characterized by X-ray absorption spectroscopy at 20 K and room temperature, Biochemistry 44 (2005) 1894–1908.
[26] J. Messinger, J.H. Robblee, U. Bergmann, C. Fernandez, P. Glatzel, H. Visser, R.M. Cinco, K.L. McFarlane, E. Bellacchio, S.A. Pizarro, S.P. Cramer, K. Sauer, M.P. Klein, V.K. Yachandra, Absence of Mn-centered oxidation in the $S_2 \rightarrow S_3$ transition: implications for the mechanism of photosynthetic water oxidation, J. Am. Chem. Soc. 123 (2001) 7804–7820.
[27] K.A. Åhrling, M.C.W. Evans, J.H.A. Nugent, R.J. Pace, The two forms of the S_2 state multiline signal in Photosystem II: effect of methanol and ethanol, Biochim. Biophys. Acta 1656 (2004) 66–77.
[28] J.L. Zimmermann, A.W. Rutherford, Electron-paramagnetic resonance properties of the S_2 state of the oxygen-evolving complex of Photosystem-II, Biochemistry 25 (1986) 4609–4615.
[29] R.J. Pace, P. Smith, R. Bramley, D. Stehlik, EPR saturation and temperature-dependence studies on signals from the oxygen-evolving center of Photosystem-II, Biochim. Biophys. Acta 1058 (1991) 161–170.
[30] A. Boussac, H. Kuhl, S. Un, M. Rogner, A.W. Rutherford, Effect of near-infrared light on the S_2-state of the manganese complex of Photosystem II from *Synechococcus elongatus*, Biochemistry 37 (1998) 8995–9000.
[31] A. Boussac, J.J. Girerd, A.W. Rutherford, Conversion of the spin state of the manganese complex in Photosystem II induced by near-infrared light, Biochemistry 35 (1996) 6984–6989.
[32] M.F. Charlot, A. Boussac, G. Blondin, Towards a spin coupling model for the Mn_4 cluster in Photosystem II, Biochim. Biophys. Acta 1708 (2005) 120–132.
[33] J.M. Peloquin, K.A. Campbell, D.W. Randall, M.A. Evanchik, V.L. Pecoraro, W.H. Armstrong, R.D. Britt, ^{55}Mn ENDOR of the S_2-state multiline EPR signal of Photosystem II: implications on the structure of the tetranuclear Mn cluster, J. Am. Chem. Soc. 122 (2000) 10926–10942.
[34] R. Baxter, E. Krausz, T. Wydrzynski, R.J. Pace, Identification of the near-infrared absorption band from the Mn cluster of Photosystem II, J. Am. Chem. Soc. 121 (1999) 9451–9452.
[35] P.J. Smith, S. Peterson, V.M. Masters, T. Wydrzynski, S. Styring, E. Krausz, R.J. Pace, Magneto-optical measurements of the pigments in fully active Photosystem II core complexes from plants, Biochemistry 41 (2002) 1981–1989.
[36] A. Boussac, M. Sugiura, D. Kirilovsky, A.W. Rutherford, Near-infrared-induced transitions in the manganese cluster of Photosystem II: action spectra for the S_2 and S_3 redox states, Plant Cell Physiol. 46 (2005) 837–842.
[37] H. Dau, L. Iuzzolino, J. Dittmer, The tetra-manganese complex of Photosystem II during its redox cycle—X-ray absorption results and mechanistic implications, Biochim. Biophys. Acta 1503 (2001) 24–39.
[38] J.H. Robblee, R.M. Cinco, V.K. Yachandra, X-ray spectroscopy-based structure of the Mn cluster and mechanism of photosynthetic oxygen evolution, Biochim. Biophys. Acta 1503 (2001) 7–23.
[39] T.G. Carrell, A.M. Tyryshkin, G.C. Dismukes, An evaluation of structural models for the photosynthetic water-oxidizing complex derived from spectroscopic and X-ray diffraction signatures, J. Biol. Inorg. Chem. 7 (2002) 2–22.
[40] Y. Kimura, N. Mizusawa, T. Yamanari, A. Ishii, T. Ono, Structural changes of D1 C-terminal alpha-carboxylate during S-state cycling in photosynthetic oxygen evolution, J. Biol. Chem. 280 (2005) 2078–2083.
[41] R.J. Debus, M.A. Strickler, L.M. Walker, W. Hillier, No evidence from FTIR difference spectroscopy that aspartate-170 of the D1 polypeptide ligates a manganese ion that undergoes oxidation during the S_0 to S_1, S_1 to S_2, or S_2 to S_3 transitions in Photosystem II, Biochemistry 44 (2005) 1367–1374.
[42] J. Cohen, K. Kim, P. King, M. Seibert, K. Schulten, Finding gas diffusion pathways in proteins: application to O_2 and H_2 transport in Cpl [FeFe]-hydrogenase and the role of packing defects, Structure 13 (2005) 1321–1329.
[43] J. Cohen, K. Kim, M. Posewitz, M.L. Ghirardi, K. Schulten, M. Seibert, P. King, Molecular dynamics and experimental investigation of H_2 and O_2 diffusion in [Fe]-hydrogenase, Biochem. Soc. Trans. 33 (2005) 80–82.
[44] J.W. Murray, J. Barber, Identification of a calcium-binding site in the PsbO protein of Photosystem II, Biochemistry 45 (2006) 4128–4130.
[45] H. Ishikita, W. Saenger, B. Loll, J. Biesiadka, E.W. Knapp, Energetics of a possible proton exit pathway for water oxidation in Photosystem II, Biochemistry 45 (2006) 2063–2071.
[46] J. Messinger, Evaluation of different mechanistic proposals for water oxidation in photosynthesis on the basis of Mn_4O_xCa structures for the catalytic site and spectroscopic data, Phys. Chem. Chem. Phys. 6 (2004) 4764–4771.
[47] J.M. Anderson, Does functional Photosystem II complex have an oxygen channel? FEBS Lett. 488 (2001) 1–4.
[48] J. Barber, J. Nield, E.P. Morris, B. Hankamer, Subunit positioning in Photosystem II revisited, Trends Biochem. Sci. 24 (1999) 43–45.
[49] A.W. Rutherford, Photosystem II, the water-splitting enzyme, Trends Biochem. Sci. 14 (1989) 227–232.
[50] M. Sivaraja, J. Tso, G.C. Dismukes, A calcium-specific site influences the structure and activity of the manganese cluster responsible for photosynthetic water oxidation, Biochemistry 28 (1989) 9459–9464.
[51] A. Boussac, J.L. Zimmermann, A.W. Rutherford, J. Lavergne, Histidine oxidation in the oxygen-evolving Photosystem II enzyme, Nature 347 (1990) 303–306.
[52] A. Boussac, J.L. Zimmermann, A.W. Rutherford, Factors influencing the formation of modified S_2 EPR signal and the S_3 EPR signal in Ca^{2+}-depleted Photosystem II, FEBS Lett. 277 (1990) 69–74.
[53] R. Mei, C.F. Yocum, Inorganic ions affect reductant-mediated inhibition of the manganese cluster of PSII, in: M. Baltscheffsky (Ed.), Current

Research in Photosynthesis, vol. I, Kluwer Academic Publishers, The Netherlands, 1990, pp. 729–732.
[54] J. Tso, M. Sivaraja, G.C. Dismukes, Calcium limits substrate accessibility or reactivity at the manganese cluster in photosynthetic water oxidation, Biochemistry 30 (1991) 4734–4739.
[55] T. Wydrzynski, W. Hillier, J. Messinger, On the functional significance of substrate accessibility in the photosynthetic water oxidation mechanism, Physiol. Plant. 96 (1996) 342–350.
[56] W.G. Gregor, R.M. Cinco, H. Yu, V.K. Yachandra, R.D. Britt, Influence of the 33 kDa manganese-stabilizing protein on the structure and substrate accessibility of the oxygen-evolving complex of Photosystem II, Biochemistry 44 (2005) 8817–8825.
[57] W. Hillier, T. Wydrzynski, Substrate water interactions within the Photosystem II oxygen evolving complex, Phys. Chem. Chem. Phys. 6 (2004) 4882–4889.
[58] W. Hillier, T. Wydrzynski, The affinities for the two substrate water binding sites in the O_2 evolving complex of Photosystem II vary independently during S-state turnover, Biochemistry 39 (2000) 4399–4405.
[59] A. Boussac, J.L. Zimmermann, A.W. Rutherford, EPR signals from modified charge accumulation states of the oxygen evolving enzyme in Ca^{2+}-deficient Photosystem II, Biochemistry 28 (1989) 8984–8989.
[60] C.X. Zhang, Interaction between tyrosine$_Z$ and substrate water in active Photosystem II, Biochim. Biophys. Acta 1757 (2006) 781–786.
[61] B. Svensson, I. Vass, E. Cedergren, S. Styring, Structure of donor side components in Photosystem II predicted by computer modeling, EMBO J. 9 (1990) 2051–2059.
[62] B. Svensson, I. Vass, S. Styring, Sequence-analysis of the D1 and D2 reaction center proteins of Photosystem II, Z. Naturforsch., C: Biosci. 46 (1991) 765–776.
[63] I. Hofacker, K. Schulten, Oxygen and proton pathways in cytochrome *c* oxidase, Proteins 30 (1998) 100–107.
[64] K. Murata, K. Mitsuoka, T. Hirai, T. Walz, P. Agre, J.B. Heymann, A. Engel, Y. Fujiyoshi, Structural determinants of water permeation through aquaporin-1, Nature 407 (2000) 599–605.
[65] B.L. de Groot, H. Grubmuller, Water permeation across biological membranes: mechanism and dynamics of aquaporin-1 and GlpF, Science 294 (2001) 2353–2357.
[66] B.L. de Groot, T. Frigato, V. Helms, H. Grubmuller, The mechanism of proton exclusion in the aquaporin-1 water channel, J. Mol. Biol. 333 (2003) 279–293.
[67] P. Brzezinski, P. Adelroth, Design principles of proton-pumping haem-copper oxidases, Curr. Opin. Struct. Biol. 16 (2006) 465–472.